

Towards Evading the Limits of Randomized Smoothing: A Theoretical Analysis

Raphael Ettetdgui^{*1}, Alexandre Araujo^{*2}, Rafael Pinot³, Yann Chevaleyre¹, Jamal Atif¹

¹ LAMSADE, Université Paris-Dauphine, CNRS, PSL University

² INRIA, Ecole Normale Supérieure, CNRS, PSL University

³ DCL, School of Computer and Communication Sciences, EPFL, Switzerland

Abstract

Randomized smoothing is the dominant standard for provable defenses against adversarial examples. Nevertheless, this method has recently been proven to suffer from important information theoretic limitations. In this paper, we argue that these limitations are not intrinsic, but merely a byproduct of current certification methods. We first show that these certificates use too little information about the classifier, and are in particular blind to the local curvature of the decision boundary. This leads to severely sub-optimal robustness guarantees as the dimension of the problem increases. We then show that it is theoretically possible to bypass this issue by collecting more information about the classifier. More precisely, we show that it is possible to approximate the optimal certificate with arbitrary precision, by probing the decision boundary with several noise distributions. Since this process is executed at certification time rather than at test time, it entails no loss in natural accuracy while enhancing the quality of the certificates. This result fosters further research on classifier-specific certification and demonstrates that randomized smoothing is still worth investigating. Although classifier-specific certification may induce more computational cost, we also provide some theoretical insight on how to mitigate it.

1 Introduction

Modern day machine learning models are vulnerable to adversarial examples, *i.e.*, small perturbations to their inputs that force misclassification [13, 37, 14]. Although a considerable amount of work has been devoted to mitigating their impact [14, 19, 25, 6, 43, 42, 3, 32, 33, 30, 31, 1, 2, 26, 23, 40, 35, 36, 12, 45, 38], defending a model against these malicious inputs remains very challenging. This difficulty to successfully resist adversarial attacks essentially comes from the difficulty to evaluate the defense mechanisms. In fact, several works have shown that it is of paramount importance to evaluate the reliability of defense mechanisms even in the worst-case scenario, *i.e.*, against a strong and adaptive attack [39, 7]. Given that it is in general intractable to build an optimal attack for a given classifier, the community now favors *certified defenses* that provide provable robustness guarantees. Among existing certification techniques, *randomized smoothing*, first introduced in [20] and refined in [22, 9, 34], has emerged as a dominant standard. In short, randomized smoothing applies a convolution between a base classifier and a Gaussian distribution to enhance the robustness of the classifier. This technique has the advantage of offering provable robustness guarantees. Formally, for any given input, we can guarantee that within a radius of this input, the classifier cannot change prediction. The maximal size of this radius is called the *certification radius* of the point. Beyond Gaussian, this technique has been generalized and can now be studied under a large class of smoothing distributions [46]. In short, randomized smoothing is considered the state-of-the-art for provable robustness for multiple classification tasks, among which image classification and segmentation [11].

* Equal contributions

Limitations of Randomized Smoothing. However, this scheme does not provide certification for free. In fact, it presents a trade-off in that using a distribution with a higher variance leads to more robust models, but at the cost of a reduction in standard accuracy. Evaluating the maximum accuracy that a certified method can achieve for a target certified radius is therefore crucial to assess the viability of this method. In this respect, several recent works support the argument that for a given probability distribution, the maximum radius that can be certified vanishes as the dimension of the learning problem increases [4, 15, 18, 46, 28, 44]. Specifically, Blum et al. [4] have shown that to successfully certify high-dimensional images, a ℓ_p -smoothing distributions must have such a large variance that it leads to a trivial classifier. This seems to make the problem of simultaneously achieving robustness and accuracy unfeasible. Building upon this first observation Hayes [15] demonstrated a similar result for *location-scale distribution* (which include the generalized Gaussian distributions) but their use of the KL divergence makes the bound loose. A tighter bound has recently been devised by Kumar et al. [18] showed that the largest ℓ_p -certification radius for some specific class of smoothing distributions decreases with rate $\mathcal{O}(1/d^{\frac{1}{2}-\frac{1}{p}})$ where d is the dimension of the images. This result was further generalized by Yang et al. [46]. Along the same line, Wu et al. [44] demonstrated an equivalent result for $p > 2$ for *spherical symmetric distributions* and a tight bound for ℓ_2 -certification radius. From an information-theoretic perspective, these results suggest that random smoothing is a doomed method for high-dimensional learning problems. This may lead some in the community to consider this method irrelevant in many modern machine learning tasks.

Closely Related Work. Two recent works [10, 27] have started exploring the lead of new certification methods, by using additional information on the classifier. For instance, Dvijotham et al. [10] use the full probability distribution at each point instead of just the probability of the dominant class. They combine this approach with an alternative to the Neyman-Pearson certification, namely relaxing the attack constraint using f -divergences, and manage to obtain slightly better certificates than existing certification methods. Similarly, Mohapatra et al. [27] and Levine et al. [21] showed that using first-order or second-order information leads to better certified radius. Mohapatra et al. also shows that it is theoretically possible to reconstruct a Gaussian smoothed classifier using only information about its successive derivatives at the point of interest (even the first derivatives are, however, extremely expensive to compute).

Our contributions. In this paper, we provide a theoretical analysis of the certification process for randomized smoothing. We advocate that current limitations are not intrinsic to the scheme, but a byproduct of current certification methods. To do so, we first focus on the uniform distribution, and provide a framework to dissociate the information-gathering process (and so the certification) from the smoothing itself, whereas current certificates use the same noise distribution for both. This makes it possible to increase the quality of the certificates without affecting the standard accuracy. Our main findings can be summarized as follows.

1. To exhibit the role of the local curvature on the quality of the certificate, we focus our study on two types of decision boundaries: cones of revolution and 2-piecewise linear. For these two types of boundaries, we quantify the gap between current certificates and the optimal one that randomized smoothing could provide. This validates our hypothesis by showing that the steeper the local curvature, the more suboptimal the certification. We also see that the gap becomes wider as the dimension grows, thus explaining the current limitations.
2. Secondly, we show that the generalized Neyman-Pearson Lemma can be used to improve the quality of certificates by collecting information from several noise distributions at the same time. By separating this information-gathering step from the smoothing itself, better certification radius can be obtained without any further loss in standard accuracy, thus circumventing the current information theoretic limitations.
3. Finally, we show that using this framework, it is possible to approximate the perfect certificate, for any decision boundaries, with arbitrary precision using information from a finite number of distributions. Although our proof requires a number of noises that increases exponentially with the dimension, we show that it is possible to drastically reduce the number of noises required when prior information is available on the classifier. We also provide several insights into the certification design process, especially computational issues, by providing techniques for reducing the dimension of the Neyman-Pearson set. More precisely, we show that it is possible to compute certificates without sampling in high-dimension by combining uniform and Gaussian distribution and leveraging the isotropic properties of the latter.

2 General framework for Randomized Smoothing

Let $\mathcal{X} = \mathbb{R}^d$ be our input space and $\mathcal{Y} = \{0, 1\}$ our label space. Let \mathcal{H} be the class of measurable functions from \mathcal{X} to \mathcal{Y} , and $h \in \mathcal{H}$ be a base classifier. Randomized smoothing creates a new classifier h_{q_0} by averaging h under some probability density function q_0 over \mathcal{X} . When receiving an input $x \in \mathcal{X}$, we compute the probability that h takes value 1 for a point drawn from $q_0(\cdot - x)$:

$$p(x, h, q_0) = \int h(z)q_0(z - x) dz$$

The smoothed classifier then returns the most probable class.

Definition 1. *The q_0 -randomized smoothing of h is the classifier:*

$$h_{q_0} : x \mapsto \mathbb{1} \left\{ p(x, h, q_0) > \frac{1}{2} \right\}$$

In the rest of the paper, we will consider the points x such that $p(x, h, q_0) > \frac{1}{2}$, so where the smoothed classifier returns 1. The other case is exactly symmetrical. An adversarial attack $\delta \in \mathcal{X}$ is a small crafted perturbation, such that $\|\delta\| \leq \epsilon$ where ϵ is a small constant and $\|\cdot\|$ is the Euclidean norm. An adversarial attack is engineered such that:

$$h_{q_0}(x + \delta) \neq y,$$

meaning $p(x + \delta, h, q_0) \leq \frac{1}{2}$. In the following, we will define the robustness guarantee provided by randomized smoothing.

Definition 2 (ϵ -certificate). *An ϵ -certificate for the q_0 -randomized smoothing of h at point x is any lower bound on the probability after attack, i.e., some value $v \in \mathbb{R}$ such that:*

$$v \leq \inf_{\delta \in B(0, \epsilon)} p(x + \delta, h, q_0)$$

A certificate v is said to be successful if $v > \frac{1}{2}$.

A successful ϵ -certificate means that no attack of norm at most ϵ can fool the classifier. This definition allows us to compare different certificates for the same smoothed classifier.

Certificates for randomized smoothing are usually “black-box”, i.e. we can only access the classifier h through limited queries. This means giving a bound on the worst-case scenario for some class of functions \mathcal{G} that we know contains h .

Definition 3 (Noised-based certificate). *Let \mathcal{Q} be a finite family of probability density functions. Let $q_0 \in \mathcal{Q}$. The \mathcal{Q} -noise-based ϵ -certificate for the q_0 -randomized smoothing of h at point x is:*

$$\text{NC}(h, q_0, x, \epsilon, \mathcal{Q}) = \inf_{g \in \mathcal{G}_{\mathcal{Q}}} \inf_{\delta \in B(0, \epsilon)} p(x + \delta, g, q_0)$$

where:

$$\mathcal{G}_{\mathcal{Q}} = \{g \in \mathcal{H} \mid \forall q \in \mathcal{Q}, p(x, g, q) = p(x, h, q)\}$$

A noise-based certificate is a lower bound over all classifiers that exhibit the same response as h to every noise distribution in \mathcal{Q} . The certificate from Cohen et al. [9] is a particular type of noise-based certificate, where we only use one distribution to gather information, namely the same q_0 that is used for the smoothing, i.e., $\mathcal{Q} = \{q_0\}$.

Note that there is a fundamental difference between q_0 , the noise used for the smoothing, which is a part of the smoothed classifier h_{q_0} used at test time, and the family \mathcal{Q} , which are noises used to analyze the base classifier h . Noises from \mathcal{Q} are only used for information-gathering.

To evaluate the quality of this certificate, we now need a benchmark. For that, we will use the *perfect certificate*, i.e., the tightest possible bound, that uses full information over the classifier h .

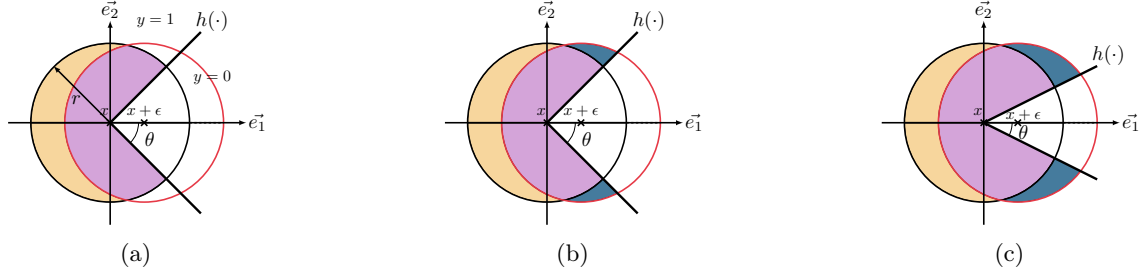


Figure 1: Illustration of Theorem 1. Figure (a) describes the probability $p(x, h, q_r) = q_r(\bullet) + q_r(\bullet)$. Figure (b) describes the perfect certificate as $\text{PC}(h, q_r, x, \epsilon) = q_r(\bullet) + q_r(\bullet)$ whereas the single noised-based certificate is $\text{NC}(h, q_r, x, \epsilon, \{q_r\}) = q_r(\bullet)$. Figure (c) shows that blue zone increases with θ , also, for $\theta = 0$, we have $q_r(\bullet) \xrightarrow{d \rightarrow \infty} 1$.

Definition 4 (Perfect certificate). *The perfect ϵ -certificate for the q_0 -randomized smoothing of h at point x is:*

$$\text{PC}(h, q_0, x, \epsilon) = \inf_{\delta \in B(0, \epsilon)} p(x + \delta, h, q_0)$$

The underestimation between perfect certificates and noise-based certificates can now be defined as the difference between both bounds.

Definition 5 (Underestimation of a noise-based certificate). *Let \mathcal{Q} be a finite family of probability density functions and let $q_0 \in \mathcal{Q}$ and $\epsilon > 0$. We define the underestimation function ν as:*

$$\nu(h, q_0, x, \epsilon, \mathcal{Q}) = \text{PC}(h, q_0, x, \epsilon) - \text{NC}(h, q_0, x, \epsilon, \mathcal{Q})$$

The function ν computes the difference between the perfect ϵ -certificate and the noise-based ϵ -certificate for an classifier h with randomized smoothing q_0 .

3 Limitations of current certificates

In this section, we provide insight on the limitation of randomized smoothing. Recall that single-noise certificates, *i.e.*, $\text{NC}(h, q_0, x, \epsilon, \{q_0\})$, use the same noise q_0 for smoothing and information-gathering. However, this technique presents several weaknesses:

1. Since \mathcal{Q} is small, the certificate is obtained as a worst-case over a large set of functions \mathcal{G} . This will often make it significantly poorer than the optimal certificate PC for our specific classifier.
2. With this kind of certificate, we have limited possibilities of optimization for the choice of the base classifier h . In particular, current certificates are blind to the “local curvature” of the decision boundary, as will be illustrated shortly.
3. Since the distribution used for the smoothing and information-gathering operations is the same. This means that a larger variance leads to more information on the decision frontier (and thus to better certificates) but at the cost of a loss of standard accuracy.

3.1 Theoretical analysis with toy decision boundaries

To illustrate these limitations, we provide a deeper analysis of the underestimation function defined in Definition 5. In the following, we focus on the case of uniform noise distributions on an ℓ_2 ball.

Intuition of Theorem 1. *For both conical and 2-piecewise-linear decision boundaries, the gap between uniform single-noise certificates and the uniform perfect certificate increases with the local curvature of the decision boundary. For high local curvatures, this gap becomes arbitrarily large as the dimension of the problem increases. Figure 1 illustrate this result in 2 dimensions.*

Theorem 1 (Underestimation of single noise-based certificates). Let $\epsilon, r \in \mathbb{R}_+^*$ such that $\epsilon \leq r$. Let $\mathcal{Q} = \{q_0\}$ where q_0 is a uniform distribution over an ℓ_2 ball $B_2^d(0, r)$. We denote $\theta_m = \arccos(\frac{\epsilon}{2r})$. For any $\theta \in [0, \theta_m]$, we denote by h_θ the classifier whose decision boundary is a cone of revolution of peak 0, axis e_1 and angle θ where (e_1, \dots, e_d) be any orthonormal basis of \mathbb{R}^d . Then, $\nu(h_\theta, q_0, 0, \epsilon, \mathcal{Q})$ is a continuous and decreasing function of θ . Furthermore, we have

- $\nu(h_0, q_0, 0, \epsilon, \mathcal{Q}) = 1 - I_{1 - (\frac{\epsilon}{2r})^2}(\frac{d+1}{2}, \frac{1}{2})$
- $\nu(h_{\theta_m}, q_0, 0, \epsilon, \mathcal{Q}) = 0$

where $I_z(a, b)$ is the incomplete regularized beta function. Furthermore, for any ϵ, r , $\nu(h_0, q_0, 0, \epsilon, \mathcal{Q}) \xrightarrow{d \rightarrow \infty} 1$. The same result holds for 2-piecewise linear sets.

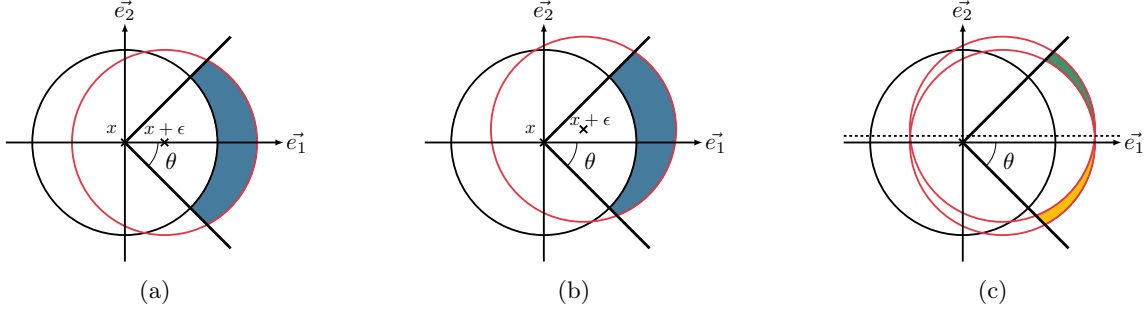


Figure 2: Illustration of the optimal attack with a cone of revolution as decision boundary. The optimal attack of norm ϵ is the vector $\delta = [\epsilon e_1, 0, \dots, 0]$. Figure (a) shows that there is always a gain by translating along e_1 , Figure (b) shows the gain when translating along both e_1 and e_2 , and finally, Figure (c) shows the difference. The loss incurred by the second translation, visible in the yellow zone, is greater than the gain (green zone). The argument of the proof is that the reflection of the blue zone through the dotted hyperplane is contained in the yellow zone.

Sketch of proof of Theorem 1. First, in order to define the perfect certificate, we show that the optimal attack against a conical decision boundary is the translation along its axis. This means that the attack defined by $\delta = [\epsilon e_1, 0, \dots, 0]^T$ is optimal. To prove that, we exploit the symmetry of the problem, as illustrated in Figure 2. To compute the difference between the perfect certificate and single-noise certificate, we here again used the rotational symmetry of the problem around axis e_1 , to compute the volume in *hyper-cylindrical coordinates* as defined Definition 7. \square

As the uniform distribution has a finite support, the corresponding single-noise certificates will be blind to everything outside that support. It will thus always consider the worst-case scenario, namely that every point outside the ball is of the opposite class. Since it has no information on the precise repartition of points in the ball, the single-noise certificate will also assume that every point “lost” after the translation (see the green left crescent zone outside the intersection in Section 3.1) was of class 1.

Hence, the difference between the perfect certificate and the single-noise certificate is the relative area of the blue zone. The last part of the result shows that as the dimension gets higher, the single noise certificate can become arbitrarily bad. In the extreme case ($\nu(\theta) = 1$), it returns 0 even though the classification task is trivial. This is due to the fact that the volume of balls tends to concentrate on their surface in high dimensions, and so the relative weight of the

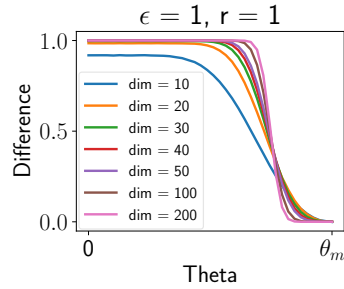


Figure 3

crescent zone increases. We used simulations to plot the evolution of the underestimation with the parameter θ and the dimension. We used Monte Carlo sampling with 200k samples for each θ and each dimension. As we can see in Figure 3, as dimension increases the cone represents a smaller portion of the space for a given θ . It follows that the underestimation becomes large for almost every θ in high dimensions. However, how likely are we to encounter these kinds of high local curvature situations for models trained on real datasets?

3.2 Empirical analysis with real-world decision boundaries

In the following, we show that we can identify the points where the single-noise classifier is suboptimal, by leveraging the information from several concentric noises. More precisely, for the uniform distribution, at points where the single-noise certificate is optimal, the probability of being in class 1 will decrease as the radius of the noise increases.

***Intuition of Proposition 1.** For an unknown decision boundary, at any point where the single-noise certificate is optimal, the probability must locally decrease with the radius of the noise. It follows that at any point where the probability increases with the radius of the noise, the single-noise certificate cannot be optimal.*

Proposition 1 (Identifying points of non-zero underestimation). For any $r > 0$, let q_r denote the uniform distribution over $B_2^d(0, r)$. Let $r_1 > 0$, and h a classifier. For any $x \in \mathbb{R}^d$, $\epsilon > 0$, if $p(x, h, q_r)$ is not a decreasing function of r over $[r_1, r_1 + \epsilon)$, then $\text{PC}(h, q_{r_1}, x, \epsilon) > \text{NC}(h, q_{r_1}, x, \epsilon, \{q_r\})$.

Suboptimality in current models. We leverage Proposition 1 to evaluate the number of points where single-noise certificates might be optimal, by “probing” the decision boundary with different distributions. Let q_0 and q_1 be two uniform distributions with r_0 and r_1 as their respective radius such that $r_0 < r_1$ and let \mathcal{D} the set containing all the images of the CIFAR10 dataset [17]. We aim at computing the proportion ζ of points where the probability increases with the radius of the noise:

Table 1

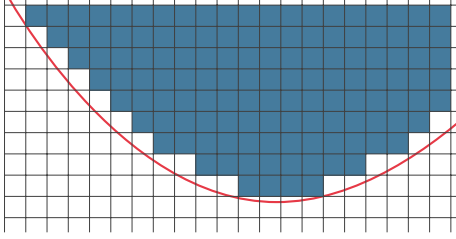
r_0 / r_1	$\zeta(r_0, r_1)$
0.25 / 0.30	40.9%
0.50 / 0.55	41.9%
0.75 / 0.80	41.3%

$$\zeta(r_0, r_1) = \frac{1}{|\mathcal{D}|} \sum_{x \in \mathcal{D}} \mathbb{1} \{p(x, h, q_0) < p(x, h, q_1)\}$$

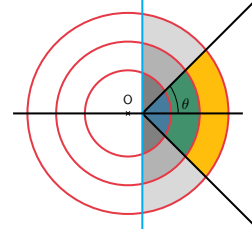
This quantity measures the proportion of points where a better information-gathering scheme could improve the certificate. In the context of randomized smoothing, it is common practice to also add noise during training in order to avoid distribution shift at test time. Therefore, to perform this experiment, we use three models trained by Yang et al. [46] with uniform distribution with respective radius of 0.25, 0.50 and 0.75. We use the same radius r_0 as the one used during training and we use a $r_1 = r_0 + 0.05$. Table 1 shows the results of this experiment. We observe that nearly half of the corrected classified points have the probability growing suggesting that single-noise certificates would underestimate the real bound.

4 Bypassing the limitations with noise-based information gathering

We now know that single-noise certificates can heavily underestimate the perfect one for points where the local curvature is high. This raises the question: is it possible for any noise-based certificate to bypass this issue? We answer positively to this question by showing that gathering information from more noise distributions at certification time allows to get as close as desired to the perfect certificate, at the expense of high computational cost in the general case. We then show that with more prior information on the decision boundary, the number of noises required and thus the computational cost can be drastically reduced.



(a) Illustration of Theorem 2. By querying the classifier with uniform noises on the squares of the grid, we can compute an approximation of the perfect certificate. As we refine the grid with smaller squares, the approximation becomes increasingly good, and converges to the perfect certificate.



(b) Illustration of Proposition 2. We see that the difference of volume captured between two balls (blue, green and yellow zones) grows with θ . For $\theta < \frac{\pi}{2}$, the volume growth is lower than for a hyperplane decision boundary (the cyan line) at the same distance. The difference is shown by the gray zones.

Figure 4

4.1 A framework for obtaining noise-based certificates

Lemma 1 (Generalized Neyman-Pearson lemma Chernoff and Scheffe [8]). *Let q_0, \dots, q_n be probability density functions. For any $k_1, \dots, k_n > 0$, we define the Neyman-Pearson set $\mathcal{S}_{\mathcal{K}} = \{q_0(x) \leq \sum_{i=1}^n k_i q_i(x)\}$ and the associated Neyman-Pearson function:*

$$\Phi_{\mathcal{K}} = \mathbb{1}\{\mathcal{S}_{\mathcal{K}}\}$$

Then for any function $\Phi : \mathcal{X} \rightarrow [0, 1]$ such that $\int \Phi q_i \, d\mu \geq \int \Phi_{\mathcal{K}} q_i \, d\mu$ for all $i \in \{1, \dots, n\}$, we have:

$$\int \Phi_{\mathcal{K}} q_0 \, d\mu \leq \int \Phi q_0 \, d\mu$$

The generalized Neyman-Pearson lemma can be reformulated with isotropic noises, to obtain what we call *noise-based certificates*.

Corollary 1 (Noise-based certificates). *Let $\mathcal{Q} = \{q_0, \dots, q_n\}$ be a finite family of isotropic probability density functions, of same center. Let $\epsilon > 0$, and any δ of norm ϵ . If the k_i are such that $\forall i, p(x, \Phi_{\mathcal{K}}, q_i) \leq p(x, h, q_i)$, then we have:*

$$\text{NC}(h, q_0, x, \epsilon, \mathcal{Q}) \geq p(x + \delta, \Phi_{\mathcal{K}}, q_0)$$

Furthermore, this becomes an equality if $\forall i, p(x, \Phi_{\mathcal{K}}, q_i) = p(x, h, q_i)$

This means that by choosing the k_i such that $p(x, \Phi_{\mathcal{K}}, q_i)$ is as close as possible from $p(x, h, q_i)$ while remaining lower, we can get arbitrary close to $\text{NC}(h, q_0, x, \epsilon, \mathcal{Q})$ using the Neyman-Pearson classifier $\Phi_{\mathcal{K}}$.

Note an important difference between multiple-noise certificates and single-noise ones: we use many noise distributions of varying amplitude *at certification time*, but the noise used for smoothing at test time, q_0 , remains constant. That is the strength of our framework: dissociating the information gathering process and the smoothing itself.

An advantage of this method is that since the function class \mathcal{G} can only shrink with the number of noises used, a bound obtained with several noises will always be at least as good as the one proposed by Cohen et al. [9].

4.2 Approximation results

In this part, we will show that noise-based information is enough to approximate any non-pathological classifier:

Intuition of Theorem 2. *For any continuous decision boundary, it is possible to approximate the perfect certificate with arbitrary precision, using information from a finite family of noise distributions. The size of the family used increases with the desired precision. An illustration of this theorem is shown in Figure 4a.*

Theorem 2 (General approximation theorem). *Let q_0 be the uniform noise on the ℓ_∞ ball $B_\infty(0, r)$ for some $r > 0$. For any $\epsilon > 0$, $\xi > 0$ and $x \in \mathbb{R}^d$, there exists a finite family \mathcal{Q} of probability density functions such that:*

$$\text{NC}(h, q_0, x, \epsilon, \mathcal{Q}) \geq \text{PC}(h, q_0, x, \epsilon) - \xi$$

Sketch of proof of Theorem 2. The idea of this proof is to define a grid of disjoint squares covering the space. Then, we can construct a noise-based classifier that returns 1 only on the squares that are entirely contained in the decision region, *i.e.*, a strict underestimate of the true classifier. As the grid gets thinner, the approximation will then converge to the true classifier as a Riemann sum. \square

Theorem 2 shows that it is possible to collect asymptotically perfect information on the decision boundary using only noise-based queries. The main improvement compared to the result of Mohapatra et al. [27] is that we reconstruct the base classifier itself, and not just the gaussian smoothed version of it, hence it works for any smoothing scheme. This shows that the black-box approach to randomized smoothing certification is viable, and can bypass the theoretical limitations when using several noises instead of one.

Furthermore, if we have access to some prior information on the decision boundary, it will be possible to design much more efficient noise-based information gathering schemes. In the following, we present a result demonstrating that we can obtain full information in the case of conical or 2-piecewise linear decision boundaries by using only a few concentric uniform noises.

Definition 6 (Noised-based certificate with prior information). *Let \mathcal{Q} be a finite family of probability density functions, \mathcal{F} be a family of classifiers (typically parameterized). Let $q_0 \in \mathcal{Q}$. The \mathcal{Q} -noise-based ϵ -certificate with prior information \mathcal{F} for the q_0 -randomized smoothing of h at point x is:*

$$\text{NCP}(h, q_0, x, \epsilon, \mathcal{Q}, \mathcal{F}) = \inf_{g \in \mathcal{G}_{\mathcal{Q}, \mathcal{F}}} \inf_{\delta \in B(0, \epsilon)} p(x + \delta, g, q_0)$$

where:

$$\mathcal{G}_{\mathcal{Q}, \mathcal{F}} = \{g \in \mathcal{F} \mid \forall q \in \mathcal{Q}, p(x, g, q) = p(x, h, q)\}$$

Intuition of Proposition 2. *If we know that the decision boundary is conical or 2-piecewise-linear, then its parameter θ can be perfectly identified using only the information from two concentric noises. This allows the perfect certificate to be computed as a noise-based certificate. Figure 4b is an intuitive illustration of the proposition. We can see that the volume of the cone captured by the balls is a strictly non-decreasing function of θ .*

Proposition 2 (Perfect certificate for conical decision boundaries). *Let $\theta_0 \in [0, \frac{\pi}{2}]$. Let h be a classifier whose decision boundary is the cone $C(0, \theta_0)$. Let \mathcal{F} be the family of all classifiers with a decision boundary of the form $C(0, \theta)$. Then there exists uniform noises q_1 and q_2 such that, for any noise q_0 , and any $x \in \mathbb{R}^d, \epsilon > 0$:*

$$\text{NCP}(h, q_0, x, \epsilon, \{q_1, q_2\}, \mathcal{F}) = \text{PC}(h, q_0, x, \epsilon)$$

Also, by a direct extension of Proposition 2, a small number of concentric noises are enough to obtain full information on general cones $C(c, \theta)$, in two steps:

- Evaluate the distance c to the decision boundary by finding the threshold such that $p(x, h, q(r)) \neq 1$;
- Use two noises of radius r_1 and r_2 to identify the angle θ as presented in Proposition 2.

This hints at a more general result for piecewise linear decision boundaries (which includes all neural networks with ReLUs activations): it may be possible to gather perfect information using only a limited number of concentric noises to “map” the fractures of the decision boundary.

Designing certificates thus shifts from a classifier-agnostic problem to a more classifier-specific one: any prior information on the decision boundary can help guide the choices of noises used at certification time. This also suggests that we could also choose the base classifier not only because of its efficiency, but to obtain some desirable properties that facilitate the certification process. This opens up a wide area of research.

5 Discussion on computational cost

In this section, we analyze the computational challenges of implementing noise-based certificates, and explore some avenues to reduce them. There are currently three main obstacles to computing noise-based certificates using the generalized Neyman-Pearson Lemma:

1. Computing integrals via Monte Carlo sampling in high-dimension can become very costly as this technique suffers from the curse of dimensionality.
2. When computing the integrals in high dimensions, numbers can become very small or very large, leading to computational instability.¹
3. Finally, fitting the k_i to compute the generalized Neyman-Pearson set is a hard stochastic optimization problem.

We show that we can bypass problems 1. and 2. when using Gaussian noise for information collection. Furthermore, uniform noise as an information gathering method considerably reduces problem 3, although suffering from problems 1 and 2.

Proposition 3 (*Computing the k_i for uniform noises*). *Let q_0, \dots, q_n be uniform distributions, where $n \ll d$ there are only at most 2^n possible values for the generalized Neyman-Pearson set \mathcal{S} .*

This means that the exact values of the k_i do not matter, only the possible values of the Neyman-Pearson set \mathcal{S} . The research of \mathcal{S} thus shifts from a hard optimization problem to a combinatorial problem with only at most 2^n values to try where n correspond to the number of noise and is usually much lower than the input dimension. Note that by taking $n = 1$, the certificate reduces to the single-noise certificate, and increasing the number of noises can only improve it. Also, we should remark that smart choices of noises can make that combinatorial problem easier in practice, since the support of the distributions does not necessarily intersect with each other.

Theorem 3 (Gathering information from gaussian noises). *Let q_0 be any isotropic probability distribution, $\sigma_1, \dots, \sigma_n > 0$. For $i = 1 \dots n$ let $q_i \sim \mathcal{N}(0, \sigma_i)$ be the noises used for information gathering. Let $S_{k_1 \dots k_n}$ be the corresponding Neyman-Pearson set, for any combination of parameters $k_1, \dots, k_n > 0$. Then $\mathbb{P}[\mathcal{N}(0, \sigma_i^2) \in S_{k_1 \dots k_n}]$ can be computed using a Monte Carlo sampling in dimension 2 from a χ distribution with $d - 2$ degrees of freedom.*

Sketch of proof for Theorem 3. The key of this proof is again the invariance by rotation of the generalized Neyman-Pearson set around the direction e_1 of the attack. This allows us to separate $\|z\|^2$ into two components, one along e_1 , which follows a 1-dimensional normal distribution, and one in e_1^\perp , whose norm follows a χ distribution with $d - 2$ degrees of freedom. \square

This means that whatever the noise used at smoothing time, we can easily gather information from gaussian noises, since the Neyman-Pearson set needs only be sampled in dimension 2 to fit the k_i .

6 Conclusion & Future Works

Computing the k_i . Theorem 3 successfully reduces the difficulty of the problem. However, even with those simplifications, fitting the k_i of the generalized Neyman-Pearson set remains a difficult stochastic optimization problem. Indeed, each step requires the computation of an integral via Monte Carlo sampling, and many steps may be necessary to reach the desired precision. A potential direction of research would be to use the relaxation introduced by Dvijotham et al. [10] for an easier to compute approximation of the Neyman-Pearson set. Both techniques from Yang et al. [46] to compute ordinary Neyman-Pearson sets can also be extended to our general sets, for more computational efficiency.

Choosing the base classifier h . Now that our certificates use more specific information on the classifier, it is possible to optimize the combination between the base classifier and the noise distributions used. For example, we may adjust our training to ensure that the decision boundary has the highest possible curvature,

¹For example, the volume of an ℓ_2 ball in dimension 784 (MNIST dimension) is approximately equal to $\exp(-1503.90)$.

since it is where our new certificates will shine. The work from Salman et al. [34], which combined noise injection and adversarial training [25] during the training, suggest that different training schemes can have an important impact on the certification performance. Recently, this line of research has been studied and further improvements have been devised [47, 16, 48, 41]. In the context of our framework, new training schemes could be devised to improve the local curvature at each point by adjusting the amount of noise injected.

Conclusion. We have shown that the limitations of randomized smoothing are a byproduct of the certification method, namely the combination of the smoothing and information gathering steps. We show that by dissociating the two processes, and using multiple distributions for the information gathering, it is possible to circumvent these limitations without affecting the standard accuracy of the classifier. This opens up a whole new field of classifier-specific certification, with the guarantee of always performing better than single-noise certificates, and without any additional loss in standard accuracy. Furthermore, it is now possible to optimize the choice of the base classifier, and use prior information in the certification process. Much work remains to be done, in order to actually implement certificates using this framework. The main difficulty is to compute the worst-case decision boundary, by fitting the constants k_i . This is hard to do using Monte Carlo sampling for most choices of noises. But the obstacles have now shifted from an impossibility result to computational challenges, restoring hope that randomized smoothing may someday be a definitive solution against adversarial attacks.

References

- [1] Alexandre Araujo, Laurent Meunier, Rafael Pinot, and Benjamin Negrevergne. Advocating for multiple defense strategies against adversarial examples. In *Joint European Conference on Machine Learning and Knowledge Discovery in Databases*, pages 165–177. Springer, 2020.
- [2] Alexandre Araujo, Benjamin Negrevergne, Yann Chevaleyre, and Jamal Atif. On lipschitz regularization of convolutional layers using toeplitz matrix theory. *Thirty-Fifth AAAI Conference on Artificial Intelligence*, 2021.
- [3] Anish Athalye, Nicholas Carlini, and David Wagner. Obfuscated gradients give a false sense of security: Circumventing defenses to adversarial examples. In *Proceedings of the 35th International Conference on Machine Learning*, 2018.
- [4] Avrim Blum, Travis Dick, Naren Manoj, and Hongyang Zhang. Random smoothing might be unable to certify ℓ_∞ robustness for high-dimensional images. *Journal of Machine Learning Research*, 2020.
- [5] LE Blumenson. A derivation of n-dimensional spherical coordinates. *The American Mathematical Monthly*, 67, 1960.
- [6] Nicholas Carlini and David Wagner. Towards evaluating the robustness of neural networks. In *2017 IEEE Symposium on Security and Privacy (SP)*, pages 39–57. IEEE, 2017.
- [7] Nicholas Carlini, Anish Athalye, Nicolas Papernot, Wieland Brendel, Jonas Rauber, Dimitris Tsipras, Ian Goodfellow, and Aleksander Madry. On evaluating adversarial robustness. *arXiv preprint arXiv:1902.06705*, 2019.
- [8] Herman Chernoff and Henry Scheffe. A generalization of the neyman-pearson fundamental lemma. *The Annals of Mathematical Statistics*, 1952.
- [9] Jeremy Cohen, Elan Rosenfeld, and Zico Kolter. Certified adversarial robustness via randomized smoothing. In *Proceedings of the 36th International Conference on Machine Learning*, 2019.
- [10] Krishnamurthy (Dj) Dvijotham, Jamie Hayes, Borja Balle, Zico Kolter, Chongli Qin, Andras Gyorgy, Kai Xiao, Sven Gowal, and Pushmeet Kohli. A framework for robustness certification of smoothed classifiers using f-divergences. In *International Conference on Learning Representations*, 2020.
- [11] Marc Fischer, Maximilian Baader, and Martin Vechev. Scalable certified segmentation via randomized smoothing. In *International Conference on Machine Learning*, pages 3340–3351. PMLR, 2021.
- [12] Timon Gehr, Matthew Mirman, Dana Drachler-Cohen, Petar Tsankov, Swarat Chaudhuri, and Martin Vechev. Ai2: Safety and robustness certification of neural networks with abstract interpretation. In *2018 IEEE Symposium on Security and Privacy (SP)*, pages 3–18. IEEE, 2018.
- [13] Amir Globerson et al. Nightmare at test time: Robust learning by feature deletion. In *Proceedings of the 23rd International Conference on Machine Learning*, 2006.
- [14] Ian Goodfellow, Jonathon Shlens, and Christian Szegedy. Explaining and harnessing adversarial examples. In *International Conference on Learning Representations*, 2015.
- [15] Jamie Hayes. Extensions and limitations of randomized smoothing for robustness guarantees. In *Proceedings of the IEEE/CVF Conference on Computer Vision and Pattern Recognition Workshops*, 2020.
- [16] Jongheon Jeong and Jinwoo Shin. Consistency regularization for certified robustness of smoothed classifiers. *Advances in Neural Information Processing Systems*, 33:10558–10570, 2020.

- [17] Alex Krizhevsky, Vinod Nair, and Geoffrey Hinton. Cifar-10 (canadian institute for advanced research). 2009.
- [18] Aounon Kumar, Alexander Levine, Tom Goldstein, and Soheil Feizi. Curse of dimensionality on randomized smoothing for certifiable robustness. In *Proceedings of the 37th International Conference on Machine Learning*, 2020.
- [19] Alexey Kurakin, Ian Goodfellow, and Samy Bengio. Adversarial examples in the physical world. *arXiv preprint arXiv:1607.02533*, 2016.
- [20] M. Lecuyer, V. Atlidakais, R. Geambasu, D. Hsu, and S. Jana. Certified robustness to adversarial examples with differential privacy. In *2019 IEEE Symposium on Security and Privacy (SP)*, 2018.
- [21] Alexander Levine, Aounon Kumar, Tom Goldstein, and Soheil Feizi. Tight second-order certificates for randomized smoothing, 2021.
- [22] Bai Li, Changyou Chen, Wenlin Wang, and Lawrence Carin. Certified adversarial robustness with additive noise. In *Advances in Neural Information Processing Systems*, 2019.
- [23] Qiyang Li, Saminul Haque, Cem Anil, James Lucas, Roger B Grosse, and Joern-Henrik Jacobsen. Preventing gradient attenuation in lipschitz constrained convolutional networks. In *Advances in Neural Information Processing Systems*, 2019.
- [24] Shengqiao Li. Concise formulas for the area and volume of a hyperspherical cap. *Asian Journal of Mathematics and Statistics*, 4(1):66–70, 2011.
- [25] Aleksander Madry, Aleksandar Makelov, Ludwig Schmidt, Dimitris Tsipras, and Adrian Vladu. Towards deep learning models resistant to adversarial attacks. In *International Conference on Learning Representations*, 2018.
- [26] Laurent Meunier, Blaise Delattre, Alexandre Araujo, and Alexandre Allauzen. A dynamical system perspective for lipschitz neural networks. In *International Conference on Machine Learning*, 2022.
- [27] Jeet Mohapatra, Ching-Yun Ko, Tsui-Wei Weng, Pin-Yu Chen, Sijia Liu, and Luca Daniel. Higher-order certification for randomized smoothing. In *Advances in Neural Information Processing Systems*, 2020.
- [28] Jeet Mohapatra, Ching-Yun Ko, Lily Weng, Pin-Yu Chen, Sijia Liu, and Luca Daniel. Hidden cost of randomized smoothing. In *Proceedings of The 24th International Conference on Artificial Intelligence and Statistics*, 2021.
- [29] Frank WJ Olver, Daniel W Lozier, Ronald F Boisvert, and Charles W Clark. *NIST handbook of mathematical functions hardback and CD-ROM*. Cambridge university press, 2010.
- [30] Rafael Pinot, Laurent Meunier, Alexandre Araujo, Hisashi Kashima, Florian Yger, Cedric Gouy-Pailler, and Jamal Atif. Theoretical evidence for adversarial robustness through randomization. In *Advances in Neural Information Processing Systems*, 2019.
- [31] Rafael Pinot, Raphael Ettetdgui, Geovani Rizk, Yann Chevaleyre, and Jamal Atif. Randomization matters how to defend against strong adversarial attacks. In *International Conference on Machine Learning*, pages 7717–7727. PMLR, 2020.
- [32] Aditi Raghunathan, Jacob Steinhardt, and Percy Liang. Certified defenses against adversarial examples. In *International Conference on Learning Representations*, 2018.
- [33] Aditi Raghunathan, Jacob Steinhardt, and Percy S Liang. Semidefinite relaxations for certifying robustness to adversarial examples. In *Advances in Neural Information Processing Systems*, 2018.

- [34] Hadi Salman, Jerry Li, Ilya Razenshteyn, Pengchuan Zhang, Huan Zhang, Sebastien Bubeck, and Greg Yang. Provably robust deep learning via adversarially trained smoothed classifiers. In *Advances in Neural Information Processing Systems*, 2019.
- [35] Sahil Singla and Soheil Feizi. Skew orthogonal convolutions. In *Proceedings of the 38th International Conference on Machine Learning*, 2021.
- [36] Sahil Singla, Surbhi Singla, and Soheil Feizi. Householder activations for provable robustness against adversarial attacks. *arXiv preprint arXiv:2108.04062*, 2021.
- [37] Christian Szegedy, Wojciech Zaremba, Ilya Sutskever, Joan Bruna, Dumitru Erhan, Ian Goodfellow, and Rob Fergus. Intriguing properties of neural networks. In *International Conference on Learning Representations*, 2014.
- [38] Vincent Tjeng, Kai Y. Xiao, and Russ Tedrake. Evaluating robustness of neural networks with mixed integer programming. In *International Conference on Learning Representations*, 2019.
- [39] Florian Tramèr, Nicholas Carlini, Wieland Brendel, and Aleksander Madry. On adaptive attacks to adversarial example defenses. In *Advances in Neural Information Processing Systems*, 2020.
- [40] Asher Trockman et al. Orthogonalizing convolutional layers with the cayley transform. In *International Conference on Learning Representations*, 2021.
- [41] Lei Wang, Runtian Zhai, Di He, Liwei Wang, and Li Jian. Pretrain-to-finetune adversarial training via sample-wise randomized smoothing, 2021.
- [42] Lily Weng, Huan Zhang, Hongge Chen, Zhao Song, Cho-Jui Hsieh, Luca Daniel, Duane Boning, and Inderjit Dhillon. Towards fast computation of certified robustness for relu networks. In *International Conference on Machine Learning*, 2018.
- [43] Eric Wong and Zico Kolter. Provable defenses against adversarial examples via the convex outer adversarial polytope. In *International Conference on Machine Learning*, 2018.
- [44] Yihan Wu, Aleksandar Bojchevski, Aleksei Kuvshinov, and Stephan Günnemann. Completing the picture: Randomized smoothing suffers from the curse of dimensionality for a large family of distributions. In *Proceedings of The 24th International Conference on Artificial Intelligence and Statistics*, 2021.
- [45] Kaidi Xu, Zhouxing Shi, Huan Zhang, Yihan Wang, Kai-Wei Chang, Minlie Huang, Bhavya Kailkhura, Xue Lin, and Cho-Jui Hsieh. Automatic perturbation analysis for scalable certified robustness and beyond. *Advances in Neural Information Processing Systems*, 33:1129–1141, 2020.
- [46] Greg Yang, Tony Duan, J. Edward Hu, Hadi Salman, Ilya Razenshteyn, and Jerry Li. Randomized smoothing of all shapes and sizes. In *Proceedings of the 37th International Conference on Machine Learning*, 2020.
- [47] Runtian Zhai, Chen Dan, Di He, Huan Zhang, Boqing Gong, Pradeep Ravikumar, Cho-Jui Hsieh, and Liwei Wang. Macer: Attack-free and scalable robust training via maximizing certified radius. In *International Conference on Learning Representations*, 2020.
- [48] Xingjian Zhen, Rudrasis Chakraborty, and Vikas Singh. Simpler certified radius maximization by propagating covariances. In *Proceedings of the IEEE/CVF Conference on Computer Vision and Pattern Recognition*, pages 7292–7301, 2021.

A Definitions

In the following, we will consider the dimension $d \geq 3$.

Definition 7 (Hyper-cylindrical coordinates) This is an extension of the hyperspherical coordinates, defined in Blumenson [5]). Let e_1, \dots, e_d be an orthonormal base of \mathbb{R}^d , with corresponding Euclidean coordinates (x_1, \dots, x_d) . The hyper-cylindrical coordinates of axis e_1 are the following change of variable:

$$z = x_1 \tag{1}$$

$$\rho = \sqrt{x_2^2 + \dots + x_d^2} \tag{2}$$

$$\phi_i = \operatorname{arccot} \left(\frac{x_i}{\sqrt{x_2^2 + \dots + x_i^2}} \right) \tag{3}$$

$$\phi_{d-1} = 2 \operatorname{arccot} \left(\frac{x_{d-1} + \sqrt{x_{d-1}^2 + x_d^2}}{x_d} \right) \tag{4}$$

with the following reverse transformation:

$$x_1 = z \tag{5}$$

$$x_2 = r \cos(\phi_1) \tag{6}$$

$$x_i = r \left(\prod_{i=1}^{i-2} \sin(\phi_i) \right) \cos(\phi_{i-1}) \tag{7}$$

$$x_d = r \left(\prod_{i=1}^{d-2} \sin(\phi_{i-2}) \right) \tag{8}$$

where $i \in \{2, \dots, d-1\}$. This is a bijection, where $\phi_i \in [0, \pi]$, $r \in \mathbb{R}_+$, and $\phi_{d-1} \in [0, 2\pi]$, with the convention that $\phi_k = 0$ when $x_k, \dots, x_n = 0$. Note that it is simply a change of variables to hyperspherical coordinates on the $d-1$ last variables.

Definition 8 (Incomplete Regularized Beta). Let $z \in \mathbb{R}$, $a > 0$ and $b > 0$. The Incomplete Regularized Beta Function is the function defined as:

$$I_z(a, b) = \frac{\Gamma(a+b)}{\Gamma(a)\Gamma(b)} \int_0^z t^{a-1} (1-t)^{b-1} dt \tag{9}$$

Definition 9 (ℓ_p -ball). The ℓ_p -ball of dimension d , radius $r > 0$ and center $c \in \mathbb{R}^d$ is the set:

$$B_p^d(c, r) = \{\forall x \in \mathbb{R}^d \mid \|x\|_p \leq r\} \tag{10}$$

Definition 10 (Spherical Cap of an ℓ_p -ball [24]). A spherical cap is the portion of the sphere that is cut away by an hyperplane of distance $r-a$ from the origin. The formula for the volume of the spherical cap is given by:

$$\operatorname{Vol}(\operatorname{Cap}(a, r, d)) = \frac{1}{2} \operatorname{Vol}(B_p^d(0, r)) I_{\frac{2ra-h^2}{r^2}} \left(\frac{d+1}{2}, \frac{1}{2} \right) \tag{11}$$

Definition 11 (Cone of revolution). Let $c \geq 0$. For any $x \in \mathbb{R}^d$, let $z, \rho, \phi_1, \dots, \phi_{d-2}$ be the hyper-cylindrical coordinates of axis e_1 (see Definition 7). The cone of revolution of axis e_1 , peaked at c and of angle $\theta \in [0, \frac{\pi}{2}]$ is the set $\mathcal{C}(c, \theta)$, defined by:

$$\left\{ \begin{array}{l} z \in \mathbb{R} \\ \rho \in \mathbb{R}_+ \\ \phi_1, \dots, \phi_{d-2} \in [0, \pi] \end{array} \middle| z > c \text{ and } \rho \leq z \tan \theta \right\}$$

when $\theta \leq \frac{\pi}{2}$ (convex cone), and the set:

$$\mathcal{C}(c, \theta) = \{z \geq c \text{ or } \rho \geq -z \tan(\pi - \theta)\}.$$

for the concave cone ($\theta > \frac{\pi}{2}$).

We define a classifier with conical decision boundary as $h_\theta : x \mapsto \mathbb{1}\{x \notin \mathcal{C}(c, \theta)\}$.

Definition 12 (2-piecewise Linear set). Let $c \geq 0$. Let x_1, \dots, x_n be the euclidean coordinates in the base (e_1, \dots, e_n) . The 2-piecewise linear decision region of axis e_1 and e_2 , of distance c and angle $\theta \in [0, \frac{\pi}{2}]$ is the set:

$$\left\{ x_1, \dots, x_n \in \mathbb{R} \mid x_1 > c \text{ and } \arctan\left(\frac{x_2}{x_1}\right) \in [-\theta, \theta] \right\}$$

Definition 13 (Linear half-space). Let $c \geq 0$. The half-space of translation c is, in hypercylindrical coordinates of axis e_1 , the set:

$$H(c) = \left\{ \begin{array}{l} z \in \mathbb{R} \\ \rho \in \mathbb{R}_+ \\ \phi_2, \dots, \phi_{d-1} \in [0, \pi] \end{array} \mid z > c \right\}$$

B Proofs of Section 3

B.1 Proof of Theorem 1

Theorem 1 (Underestimation of single noise-based certificates). Let $\epsilon, r \in \mathbb{R}_+^*$ such that $\epsilon \leq r$. Let $\mathcal{Q} = \{q_0\}$ where q_0 is a uniform distribution over an ℓ_2 ball $B_2^d(0, r)$. We denote $\theta_m = \arccos(\frac{\epsilon}{2r})$. For any $\theta \in [0, \theta_m]$, we denote by h_θ the classifier whose decision boundary is a cone of revolution of peak 0, axis e_1 and angle θ where (e_1, \dots, e_d) be any orthonormal basis of \mathbb{R}^d . Then, $\nu(h_\theta, q_0, 0, \epsilon, \mathcal{Q})$ is a continuous and decreasing function of θ . Furthermore, we have

- $\nu(h_0, q_0, 0, \epsilon, \mathcal{Q}) = 1 - I_{1-(\frac{\epsilon}{2r})^2}\left(\frac{d+1}{2}, \frac{1}{2}\right)$
- $\nu(h_{\theta_m}, q_0, 0, \epsilon, \mathcal{Q}) = 0$

where $I_z(a, b)$ is the incomplete regularized beta function. Furthermore, for any ϵ, r , $\nu(h_0, q_0, 0, \epsilon, \mathcal{Q}) \xrightarrow{d \rightarrow \infty} 1$. The same result holds for 2-piecewise linear sets.

Lemma 2 (Limit of the regularized incomplete beta function). Let $z \leq 1$, $b = \frac{1}{2}$ fixed. Then $I_z(a, b) \xrightarrow{a \rightarrow \infty} 0$.

Proof. For any $z < 1$, $a > 1$, $b = \frac{1}{2}$, we have:

$$I_z(a, b) = \frac{\Gamma(a+b)}{\Gamma(a)\Gamma(b)} \int_0^z t^{a-1} (1-t)^{b-1} dt \quad (12)$$

$$\leq \frac{\Gamma(a+b)}{\Gamma(a)\Gamma(b)} z^a (1-z)^{-\frac{1}{2}} \quad (13)$$

From Olver et al. [29], Equation 5.11.12, we have the following approximation:

$$\frac{\Gamma(a+b)}{\Gamma(a)} \underset{a \rightarrow +\infty}{\sim} a^b \quad (14)$$

from Equation (14), we can show that:

$$\frac{\Gamma(a+b)}{\Gamma(a)\Gamma(b)} \underset{a \rightarrow +\infty}{\sim} \frac{a^b}{\Gamma(b)} \quad (15)$$

Finally, we have:

$$I_z(a, b) \leq \frac{\Gamma(a+b)}{\Gamma(a)\Gamma(b)} z^a (1-z)^{-\frac{1}{2}} \quad (16)$$

$$\underset{a \rightarrow +\infty}{\sim} \frac{a^b}{\Gamma(b)} z^a (1-z)^{-\frac{1}{2}} \quad (17)$$

$$\xrightarrow{a \rightarrow +\infty} 0 \quad (18)$$

which concludes the proof. \square

In what follows, $V = \text{Vol}(B_2^d(0, r))$

Lemma 3. *The optimal attack of size $\epsilon < r$ against $\mathcal{C}(0, \theta)$ is the translation fully along its axis e_1 , i.e. ϵe_1 .*

Proof. Let $A = \text{Span}(e_1)$, $B = \text{Span}(e_2, \dots, e_d)$. For any vector $u \in \mathbb{R}^d$, we write $u = u_A + u_B$ where u_A and u_B are the orthogonal projections of u on A and B respectively.

First we will show that since the cone is invariant by rotation around e_1 , the orthogonal component of the attack is as well. Without any attack, the probability of returning 1 at point 0, is

$$\frac{1}{V} \int_{\mathbb{R}^d} \mathbb{1} \{ \|x_A - 0\|^2 + \|x_B - 0\|^2 \leq r^2 \} \mathbb{1} \{ \|x_B\| \leq \|x_A\| \tan(\theta) \} dx \quad (19)$$

where V is the volume of the ball of radius r and center 0.

Let δ be any attack vector, $\|\delta\| = \epsilon$. Attacking by δ amounts to shifting the center of the ball from $(0, 0)$ to (δ_A, δ_B) . Let

$$f(x, \delta) = \mathbb{1} \{ \|x_A - \delta_A\|^2 + \|x_B - \delta_B\|^2 \leq r^2 \} \mathbb{1} \{ \|x_B\| \leq \|x_A\| \tan(\theta) \}, \quad \forall x \in \mathbb{R}^d \quad (20)$$

Then the probability of returning 1 at point 0, under attack δ , is $p(\delta) = \frac{1}{V} \int_{\mathbb{R}^d} f(x, \delta) dx$ where V is independent of δ .

Now let g be any isometric mapping such that $g|_A = \text{Id}_A$. Let $\tilde{\delta} = g(\delta)$. Recall that as g is an isometry hence g and g^{-1} are also affine, hence we have

$$f(g^{-1}(x), \delta) = \mathbb{1} \{ \|g^{-1}(x_A) - \delta_A\|^2 + \|g^{-1}(x_B) - \delta_B\|^2 \leq r^2 \} \mathbb{1} \{ \|g^{-1}(x_B)\| \leq \|g^{-1}(x_A)\| \tan(\theta) \} \quad (21)$$

$$= \mathbb{1} \{ \|g^{-1}(x_A - \tilde{\delta}_A)\|^2 + \|g^{-1}(x_B - \tilde{\delta}_B)\|^2 \leq r^2 \} \mathbb{1} \{ \|g^{-1}(x_B)\| \leq \|g^{-1}(x_A)\| \tan(\theta) \} \quad (22)$$

$$= \mathbb{1} \{ \|x_A - \tilde{\delta}_A\|^2 + \|x_B - \tilde{\delta}_B\|^2 \leq r^2 \} \mathbb{1} \{ \|x_B\| \leq \|x_A\| \tan(\theta) \} \quad (23)$$

$$= f(x, \tilde{\delta}) = f(x, g^{-1}(\delta)) \quad (24)$$

since g^{-1} is an isometry. It follows, by a change of variable in the integral:

$$p(\delta) = \frac{1}{V} \int_{\mathbb{R}^d} f(x, \delta) dx \quad (25)$$

$$= \frac{1}{V} \int_{\mathbb{R}^d} f(g^{-1}(u), \delta) du \quad (26)$$

$$= \frac{1}{V} \int_{\mathbb{R}^d} f(u, g^{-1}(\delta)) du \quad (27)$$

$$= p(\tilde{\delta}) \quad (28)$$

In particular, we can always choose g such that the $g(\delta_B) = \delta_2 e_2$. In what follows, we will consider δ of the form $\delta = \delta_1 e_1 + \delta_2 e_2$ and show that the attack is optimal when $\delta_2 = 0$. For this, we will compute the difference between the attack translated by $\delta_1 e_1$ and the one translated by $\delta_1 e_1 + \delta_2 e_2$, to show that the orthogonal component actually reduces the efficiency of the attack. Let us first recall that

$$p(\delta) = \frac{1}{V} \int_{\mathbb{R}^d} \mathbb{1} \{ \|x_1 - \delta_1\|^2 + \|x_2 - \delta_2\|^2 + \|x_3\|^2 + \dots + \|x_d\|^2 \leq r^2 \} \mathbb{1} \{ \|x_B\| \leq \|x_A\| \tan(\theta) \} dx_1 \dots dx_d \quad (29)$$

$$= \frac{1}{V} \text{Vol}(B(\delta, r) \cap C(0, \theta)). \quad (30)$$

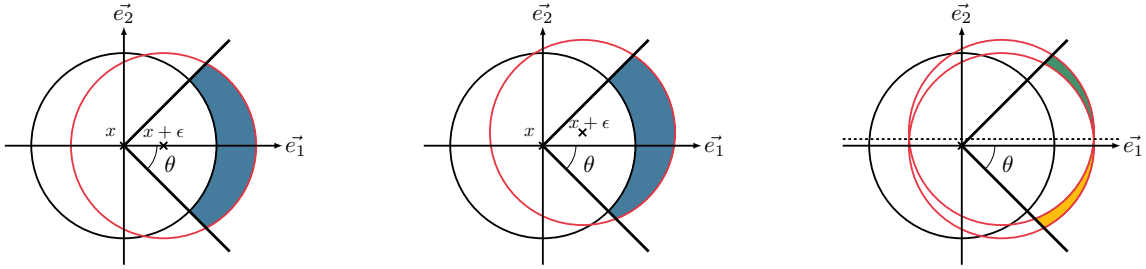


Figure 5: Illustration of the proof. The illustration on the left shows that there is always a gain by translating along e_1 , the illustration in the middle shows the gain when translating along both e_1 and e_2 , and finally, the illustration on the right shows the difference. The loss incurred by the second translation, visible in the yellow zone, is greater than the gain (green zone). The argument of the proof is that the symmetric of the blue zone is contained in the yellow zone.

Let $A = B(\delta, r) \cap C(0, \theta) \setminus B(\delta_1 e_1, r)$ and $D = B(\delta_1 e_1, r) \cap C(0, \theta) \setminus B(\delta, r)$.

$$p(\delta_1 e_1) - p(\delta) = \frac{1}{V} \text{Vol}(B(\delta, r) \cap C(0, \theta)) - \frac{1}{V} \text{Vol}(B(\delta_1 e_1, r) \cap C(0, \theta)) \quad (31)$$

$$= \frac{1}{V} (\text{Vol}(B(\delta, r) \cap C(0, \theta) \cap B(\delta_1 e_1, r)) + \text{Vol}(B(\delta, r) \cap C(0, \theta) \setminus B(\delta_1 e_1, r))) \quad (32)$$

$$- \text{Vol}(B(\delta_1 e_1, r) \cap C(0, \theta)) \cap B(\delta, r) - \text{Vol}(B(\delta_1 e_1, r) \cap C(0, \theta) \setminus B(\delta, r)) \quad (33)$$

$$= \frac{1}{V} (\text{Vol}(D) - \text{Vol}(A)) \quad (34)$$

We have $p(\delta_1 e_1) - p(\delta) = \frac{1}{V} (\text{Vol}(D) - \text{Vol}(A))$. To show that it is positive, we will show that there is an isometry v (preserving volumes) such that $v(A) \subset D$.

Let v be the reflection across the hyperplan $\{x \in \mathbb{R}^d, x_2 = \frac{\delta_2}{2}\}$. We have $v(x_1, \dots, x_d) = (x_1, \delta_2 - x_2, x_3, \dots, x_d)$. For simplicity, for any $x \in \mathbb{R}^d$, we denote $v(x) = \tilde{x}$.

Let $x \in A$. We will show that \tilde{x} is in D . As x is in A , we have

$$\begin{cases} (x_1 - \delta_1)^2 + (x_2 - \delta_2)^2 + x_3^2 + \dots + x_d^2 \leq r^2 & (35) \\ x_1 > 0 & (36) \end{cases}$$

$$x_2^2 + \dots + x_d^2 \leq x_1^2 \tan^2(\theta) \quad (37)$$

$$\begin{cases} (x_1 - \delta_1)^2 + x_2^2 + x_3^2 + \dots + x_d^2 > r^2 & (38) \end{cases}$$

Equation (35) states that $x \in B(\delta, r)$, Equation (36) and Equation (37) state that it is in the cone, whereas Equation (38) says that $x \notin B(\delta_1 e_1, r)$.

Let us first show that $\tilde{x} \in C(0, \theta)$. $\tilde{x}_1 = x_1 > 0$, and subtracting Equation (35) from Equation (38) gives us $x_2^2 > (x_2 - \delta_2)^2$. It follows:

$$\tilde{x}_2^2 + \cdots + \tilde{x}_d^2 = (\delta_2 - x_2)^2 + x_3^2 + \cdots + x_d^2 \quad (39)$$

$$< x_2^2 + \cdots + x_d^2 \quad (40)$$

$$\leq x_1^2 \tan^2(\theta) \quad (\text{from Equation (37)}) \quad (41)$$

$$= \tilde{x}_1 \tan^2(\theta) \quad (42)$$

Now we show that $\tilde{x} \in B(\delta_1 e_1, r)$.

$$(\tilde{x}_1 - \delta_1)^2 + \tilde{x}_2^2 + \cdots + \tilde{x}_d^2 = (x_1 - \delta_1)^2 + (x_2 - \delta_2)^2 + x_3^2 + \cdots + x_d^2 \quad (43)$$

$$\leq r^2 \quad (44)$$

Finally we show $\tilde{x} \notin B(\delta, r)$.

$$(\tilde{x}_1 - \delta_1)^2 + (\tilde{x}_2 - \delta_2)^2 + \cdots + \tilde{x}_d^2 = (x_1 - \delta_1)^2 + x_2^2 + x_3^2 + \cdots + x_d^2 \quad (45)$$

$$> r^2 \quad (\text{from Equation (38)}) \quad (46)$$

Combining the above, we get $\tilde{x} \in D$. As x was chosen arbitrarily in A , we get $v(A) \subset D$. As v is isometric, we finally get $p(\delta_1 e_1) - p(\delta) = \frac{1}{V} (\text{Vol}(A) - \text{Vol}(D)) = \frac{1}{V} (\text{Vol}(v(A)) - \text{Vol}(D)) \leq 0$. The component orthogonal to the axis is detrimental to the attack.

We now only need to prove that $p(\delta)$ is strictly increasing with δ_1 . For what follow, we consider an attack $\delta_1 e_1$, and another one $((\delta_1 + \Delta)e_1)$. We will use the same technique:

Let $A = B(\delta_1 e_1, r) \cap C(0, \theta) \setminus B((\delta_1 + \Delta)e_1, r)$, and $D = B((\delta_1 + \Delta)e_1, r) \cap C(0, \theta) \setminus B(\delta_1 e_1, r)$. We have $p((\delta_1 + \Delta)e_1) - p(\delta_1 e_1) = \frac{1}{V} (\text{Vol}(D) - \text{Vol}(A))$, and we will show that there is an isometry v such that $v(A) \subset D$.

Let v be the reflection across the hyperplane $\{x \in \mathbb{R}^d \mid x_1 = \delta_1 + \frac{\Delta}{2}\}$. Let $x = (x_1, \dots, x_d) \in A$. It verifies the following equations:

$$\left\{ \begin{array}{l} (x_1 - \delta_1)^2 + x_2^2 + x_3^2 + \cdots + x_d^2 \leq r^2 \end{array} \right. \quad (47)$$

$$x_1 > 0 \quad (48)$$

$$x_2^2 + \cdots + x_d^2 \leq x_1^2 \tan^2(\theta) \quad (49)$$

$$\left\{ \begin{array}{l} (x_1 - \delta_1 - \Delta)^2 + x_2^2 + x_3^2 + \cdots + x_d^2 > r^2 \end{array} \right. \quad (50)$$

$$v(x_1, \dots, x_d) = (2\delta_1 + \Delta - x_1, x_2, \dots, x_d) = \tilde{x}.$$

First of all, subtracting Equation (50) from Equation (47) gives:

$$(x_1 - \delta_1 - \Delta)^2 > (x_1 - \delta_1)^2 \Rightarrow \Delta^2 - 2\Delta(x_1 - \delta_1) > 0 \quad (51)$$

$$\Rightarrow x_1 < \delta_1 + \frac{\Delta}{2} \quad (52)$$

Let us show $\tilde{x} \in D$.

$$\tilde{x}_1^2 \tan^2(\theta) = (2\delta_1 + \Delta - x_1)^2 \tan^2(\theta) \quad (53)$$

$$\geq \left(2\delta_1 + \Delta - \delta_1 - \frac{\Delta}{2}\right)^2 \tan^2(\theta) \quad (54)$$

$$= \left(\delta_1 + \frac{\Delta}{2}\right)^2 \tan^2(\theta) \quad (55)$$

$$\geq x_1^2 \tan^2(\theta) \quad (56)$$

$$\geq x_2^2 + \cdots + x_d^2 \quad (57)$$

$$= \tilde{x}_2^2 + \cdots + \tilde{x}_d^2 \quad (58)$$

Hence $\tilde{x} \in C(0, \theta)$. Then:

$$(\tilde{x}_1 - \delta_1 - \Delta)^2 + \tilde{x}_2^2 + \cdots + \tilde{x}_d^2 = (x_1 - \delta_1)^2 + x_2^2 + \cdots + x_d^2 \quad (59)$$

$$\leq r^2 \quad (60)$$

Hence $\tilde{x} \in B((\delta_1 + \Delta)e_1, r)$. Finally,

$$(\tilde{x}_1 - \delta_1)^2 + \tilde{x}_2^2 + \cdots + \tilde{x}_d^2 = (x_1 - \delta_1 - \Delta)^2 + x_2^2 + \cdots + x_d^2 \quad (61)$$

$$> r^2 \quad (62)$$

and we have $\tilde{x} \notin B(\delta_1 e_1, r)$. We have thus shown that $\text{Vol}(D) \geq \text{Vol}(A)$, and so the attack is increasing in δ_1 . We will now show that the increase is strict. For that, we show that there exists points in D whose image by v is not in A .

Recall that $D = B(\delta_1 + \Delta, r) \cap C(0, \theta) \setminus B(\delta_1, r)$ is defined by the following set of equations:

$$\left\{ \begin{array}{l} (x_1 - \delta_1 - \Delta)^2 + x_2^2 + x_3^2 + \cdots + x_d^2 \leq r^2 \\ x_1 > 0 \end{array} \right. \quad (63)$$

$$\left\{ \begin{array}{l} x_2^2 + \cdots + x_d^2 \leq x_1^2 \tan^2(\theta) \\ (x_1 - \delta_1)^2 + x_2^2 + x_3^2 + \cdots + x_d^2 > r^2 \end{array} \right. \quad (64)$$

$$\left\{ \begin{array}{l} x_2^2 + \cdots + x_d^2 \leq x_1^2 \tan^2(\theta) \\ (x_1 - \delta_1)^2 + x_2^2 + x_3^2 + \cdots + x_d^2 > r^2 \end{array} \right. \quad (65)$$

$$\left\{ \begin{array}{l} x_2^2 + \cdots + x_d^2 \leq x_1^2 \tan^2(\theta) \\ (x_1 - \delta_1)^2 + x_2^2 + x_3^2 + \cdots + x_d^2 > r^2 \end{array} \right. \quad (66)$$

Let us reason by contradiction, and assume that $v(D) \subset A$

This means that for all points verifying the previous set of equations, we also have $x_2^2 + \cdots + x_d^2 \leq \tilde{x}_1^2 \tan^2(\theta)$, i.e.

$$x_2^2 + \cdots + x_d^2 \leq (2\delta_1 + \Delta - x_1)^2 \tan^2(\theta) \quad (67)$$

Let us define $u = x_1 - \delta$ and $b = \delta + \Delta$. Combining eq. (67) and eq. (66) gives:

$$\begin{aligned} r^2 &\leq (x_1 - \delta)^2 + (2\delta + \Delta - x_1)^2 \tan^2(\theta) \\ &\leq u^2 + (b - u)^2 \tan^2(\theta) \\ &\leq u^2 + (b^2 + u^2 - 2bu) \tan^2(\theta) \end{aligned}$$

This implies:

$$\begin{aligned} (1 + \tan^2(\theta))u^2 - 2b \tan^2(\theta)u + b^2 - r^2 &> 0 \\ \Rightarrow b^2 - r^2 &> b^2 \frac{\tan^2(\theta)}{1 + \tan^2(\theta)} \\ \Rightarrow r^2 &< b^2(1 - \sin^2(\theta) \tan^2(\theta)) \\ \Rightarrow r^2 &< \delta^2(1 - \tan^2(\theta)) \\ \Rightarrow r^2 &< \delta^2 \end{aligned}$$

Which is a contradiction since we consider attacks of size $\delta = \epsilon < r$.

We have shown that any component of the attack that is orthogonal to e_1 is detrimental to the attack, and that an increase along e_1 benefits the attack. It follows that the optimal attack of size at most ϵ is ϵe_1 . \square

Proof of Theorem 1. Let $r > 0$, $0 < \epsilon \leq r$, $\delta = [\epsilon, 0, \dots, 0]^\top \in \mathbb{R}^d$, $\theta \in [0, \theta_m]$ with $\theta_m = \arccos(\frac{\epsilon}{2r})$. Let $\mathcal{C}(0, \theta)$ be a cone of revolution of peak 0, axis e_1 and angle θ . Let us consider all functions h_θ whose decision

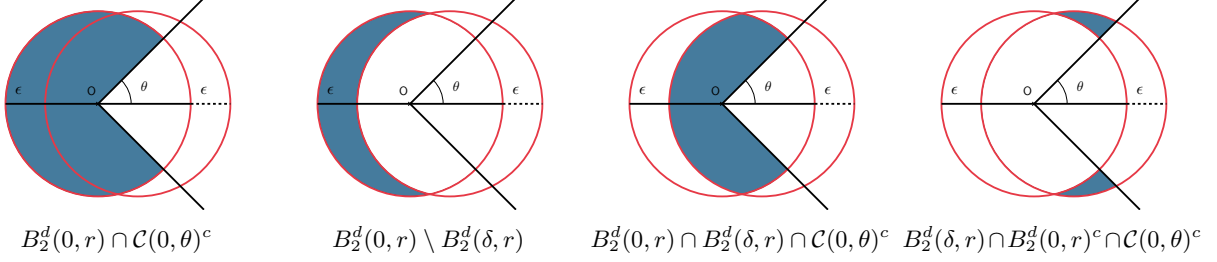


Figure 6: Illustration of proof of Theorem 1. The worst-case classifier using only the information $p(\theta)$ assumes that the zone in the second figure is entirely lost, whereas for the perfect certificate, the blue zone in the fourth figure is not lost. That zone grows as θ shrinks.

boundary is the cone of revolution $\mathcal{C}(0, \theta)$. The probability $p(x, h_\theta, q_0)$ of returning class 1 at the point 0 for the classifier h_θ after smoothing by q_0 is:

$$p(x, h_\theta, q_0) = \int_{\mathbb{R}^d} \frac{\mathbb{1}\{x \in B_2^d(0, r)\}}{\text{Vol}(B_2^d(0, r))} \mathbb{1}\{x \in \mathcal{C}(0, \theta)^c\} dx \quad (68)$$

$$= \frac{\text{Vol}(B_2^d(0, r) \cap \mathcal{C}(0, \theta)^c)}{\text{Vol}(B_2^d(0, r))} \quad (69)$$

Single-noise certificates uses the fact that in the worst-case scenario, all the volume lost during the translation was in class 1, and all the volume gained is in the class 0 (see proof of Yang et al. [46] [Theorem I.19]) This gives:

$$\text{NC}(h_\theta, q_0, x, \epsilon, \{q_0\}) = p(x, h_\theta, q_0) - \frac{1}{V} (\text{Vol}(B_2^d(0, r) \setminus B_2^d(\delta, r))) \quad (70)$$

$$= \frac{1}{V} (\text{Vol}(B_2^d(0, r) \cap \mathcal{C}(0, \theta)^c) - (\text{Vol}(B_2^d(0, r) \setminus B_2^d(\delta, r)))) \quad (71)$$

$$= \frac{1}{V} \text{Vol}(B_2^d(0, r) \cap B_2^d(\delta, r) \cap \mathcal{C}(0, \theta)^c) \quad (72)$$

In Equation (70), we say that in the worst case scenario all the volume lost during the translation was in class 1, and all volume gained was in class 0, hence we loose everything outside the intersection.

This corresponds to Appendix B.1: the zone that is preserved after translation for the noise certificate is the blue one in the third figure. We will show that the perfect certificate also preserves the blue zone in the fourth figure.

Since by Lemma 3 the optimal attack against the cone is the translation along its axis, the perfect certificate for the probability p will be defined under the attack δ :

$$\text{PC}(h_\theta, q_0, x, \epsilon) = \frac{1}{V} \text{Vol}(B_2^d(\delta, r) \cap \mathcal{C}(0, \theta)^c) \quad (73)$$

The difference between the perfect certificate and the single-noise based certificate (as in Definition 5) is:

$$\nu(h_\theta, q_0, x, \epsilon, \{q_0\}) = \frac{1}{V} (\text{Vol}(B_2^d(\delta, r) \cap \mathcal{C}(0, \theta)^c) - \text{Vol}(B_2^d(0, r) \cap B_2^d(\delta, r) \cap \mathcal{C}(0, \theta)^c)) \quad (74)$$

$$= \frac{1}{V} \text{Vol}(B_2^d(\delta, r) \cap \mathcal{C}(0, \theta)^c \setminus (B_2^d(0, r) \cap B_2^d(\delta, r) \cap \mathcal{C}(0, \theta)^c)) \quad (75)$$

$$= \frac{1}{V} \text{Vol}(B_2^d(\delta, r) \cap \mathcal{C}(0, \theta)^c \cap (B_2^d(0, r) \cap B_2^d(\delta, r) \cap \mathcal{C}(0, \theta)^c)^c) \quad (76)$$

$$= \frac{1}{V} \text{Vol}(B_2^d(\delta, r) \cap \mathcal{C}(0, \theta)^c \cap (B_2^d(0, r)^c \cup B_2^d(\delta, r)^c \cup \mathcal{C}(0, \theta))) \quad (77)$$

$$= \frac{1}{V} \text{Vol}(B_2^d(\delta, r) \cap B_2^d(0, r)^c \cap \mathcal{C}(0, \theta)^c) \quad (78)$$

$$= \frac{A}{V} \int_{x=0}^{\infty} \int_{\rho=x \tan(\theta)}^{\infty} \mathbb{1}\{(x-\epsilon)^2 + \rho^2 \leq r^2\} \mathbb{1}\{x^2 + \rho^2 > r^2\} \rho^{d-2} dx d\rho \quad (79)$$

where $A = \int_{\substack{\phi_1, \dots, \phi_{d-3} \in [-\pi, \pi] \\ \phi_{d-2} \in [0, 2\pi]}} \prod_{k=1}^{d-2} \sin^k \phi_{d-1-k} d\phi_1 \dots d\phi_{d-2}$.

It follows that ν is a continuous function with respect to $\theta \in [0, \theta_m]$. It is decreasing, since $\mathcal{C}(0, \theta_1) \subset \mathcal{C}(0, \theta_2)$ when $\theta_1 < \theta_2$.

Furthermore, when $\theta = 0$:

$$\nu(h_0, q_0, x, \epsilon, \{q_0\}) = \frac{1}{V} \text{Vol}(B_2^d(\delta, r) \cap B_2^d(0, r)^c) \quad (80)$$

$$= \frac{1}{V} \text{Vol}(B_2^d(\delta, r) \setminus B_2^d(0, r)) \quad (81)$$

$$= \frac{1}{V} \text{Vol}(B_2^d(\delta, r)) - \text{Vol}(B_2^d(0, r) \cap B_2^d(\delta, r)) \quad (82)$$

$$= \frac{1}{V} \left(\text{Vol}(B_2^d(\delta, r)) - 2 \text{Vol}(\text{Cap}(r - \frac{\epsilon}{2}, r, d)) \right) \quad (83)$$

$$= 1 - I_{1 - (\frac{\epsilon}{2r})^2} \left(\frac{d+1}{2}, \frac{1}{2} \right) \quad (84)$$

where the step from Equation (82) to Equation (83) is due because the intersection of both spheres is the union of two spherical caps.

Moreover, from Lemma 2, we have $\nu(h_0, q_0, x, \epsilon, \{q_0\}) \xrightarrow{d \rightarrow \infty} 1$:

And, when $\theta = \theta_m$, we are going to prove that $\nu(h_{\theta_m}, q_0, x, \epsilon, \{q_0\}) = 0$. Equivalently, we want to show that the set defined by:

$$\left\{ (x, \rho) \in \mathbb{R} \mid x < \frac{\epsilon}{2} \mid (x-\epsilon)^2 + \rho^2 \leq r^2 \mid \rho > x \tan \theta_m \right\} \quad (85)$$

is an empty set. Let (x, ρ) in this set. We have:

$$\rho > x \tan \left(\arccos \left(\frac{\epsilon}{2r} \right) \right) \quad (86)$$

$$= \frac{2rx}{\epsilon} \sqrt{1 - \frac{\epsilon^2}{4r^2}} \quad (87)$$

due to the equality: $\tan(\arccos(x)) = \frac{\sqrt{1-x^2}}{x}$. Then, we have:

$$r^2 \geq (x - \epsilon)^2 + \rho^2 \quad (88)$$

$$\geq x^2 - 2x\epsilon + \epsilon^2 + \frac{4r^2x^2}{\epsilon^2} \left(1 - \frac{\epsilon^2}{4r^2}\right) \quad (89)$$

$$= x^2 - 2x\epsilon + \epsilon^2 + \frac{4r^2x^2}{\epsilon^2} - x^2 \quad (90)$$

$$= \frac{4r^2}{\epsilon^2}x^2 - 2x\epsilon + \epsilon^2 \quad (91)$$

Hence we have:

$$\frac{4r^2}{\epsilon^2}x^2 - 2x\epsilon + \epsilon^2 - r^2 \leq 0 \quad \text{and} \quad x \leq \frac{\epsilon}{2} \quad (92)$$

But the minimum of the right hand side is: $\frac{\epsilon^3}{4r^2} \leq \frac{\epsilon}{2}$ because $r \leq \epsilon$. Therefore, the r.h.s is increasing on the interval $[\frac{\epsilon}{2}, \infty]$ and is equal to 0 when $x = \frac{\epsilon}{2}$, which proves that no point verifies Equation (92). That allows us to conclude that: $\nu(h_{\theta_m}, q_0, x, \epsilon, \{q_0\}) = 0$. □

B.2 Proof of proposition 1

Proposition 1 (Identifying points of non-zero underestimation). *For any $r > 0$, let q_r denote the uniform distribution over $B_2^d(0, r)$. Let $r_1 > 0$, and h a classifier. For any $x \in \mathbb{R}^d$, $\epsilon > 0$, if $p(x, h, q_r)$ is not a decreasing function of r over $[r_1, r_1 + \epsilon)$, then $\text{PC}(h, q_{r_1}, x, \epsilon) > \text{NC}(h, q_{r_1}, x, \epsilon, \{q_r\})$.*

Proof. Recall the definition of the noised-based certificates (see Definition 3). When the infimum over $\mathcal{G}_{\mathcal{Q}}$ is attained by some g , we call g a \mathcal{Q} -worst case classifier. Now, let us denote q_r , the uniform distribution of radius $r > 0$, let $r_1 > 0$ and let $D_{r_1} = \{z \in \mathcal{X} \mid g_{r_1}(z) = 1\}$, a half-space. As we saw in the proof of Theorem 1, for any δ of norm ϵ , the $\{q_{r_1}\}$ -worst classifier g_{r_1} has a decision region D_{r_1} that is entirely contained in $B_2^d(x, r_1)$. Hence for any $r > r_1$,

$$p(x, g_{r_1}, q_r) = \mathbb{P}[U(x, r) \in D_{r_1}] \quad (93)$$

$$= \frac{\text{Vol}(B_2^d(0, r) \cap D_{r_1})}{\text{Vol}(B_2^d(x, r))} \quad (94)$$

$$= \frac{\text{Vol}(B_2^d(x, r_1) \cap D_{r_1})}{\text{Vol}(B_2^d(x, r))} \quad (95)$$

because $B_2^d(x, r) \cap D_{r_1} \subset B_2^d(x, r_1)$. Since r_1 is constant, this is a decreasing function in r .

A similar proof works for 2-piecewise linear decision boundaries. □

B.3 Proof of Proposition 2

Proposition 2 (Perfect certificate for conical decision boundaries). *Let $\theta_0 \in [0, \frac{\pi}{2}]$. Let h be a classifier whose decision boundary is the cone $C(0, \theta_0)$. Let \mathcal{F} be the family of all classifiers with a decision boundary of the form $C(0, \theta)$. Then there exists uniform noises q_1 and q_2 such that, for any noise q_0 , and any $x \in \mathbb{R}^d$, $\epsilon > 0$:*

$$\text{NCP}(h, q_0, x, \epsilon, \{q_1, q_2\}, \mathcal{F}) = \text{PC}(h, q_0, x, \epsilon)$$

Definition 14 (Volume growth for a decision boundary). *Let B_2^d , the ℓ_2 -ball in dimension d , \mathcal{A} a set and $r_1 > r_2 \geq 0$. We define the volume growth of \mathcal{A} from r_1 to r_2 as:*

$$\Delta V(\mathcal{A}, r_1, r_2) = \text{Vol}(\mathcal{A} \cap B_2^d(0, r_2)) - \text{Vol}(\mathcal{A} \cap B_2^d(0, r_1))$$

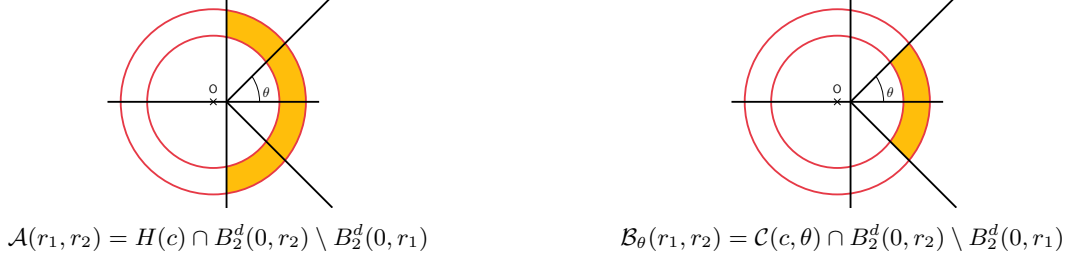


Figure 7: Illustration of the proof of Lemma 4.

Lemma 4 (Growth function for concentric noises). *Let $c \geq 0$, $r_2 > r_1 > c$. Then $\Delta V(\mathcal{C}(c, \theta), r_1, r_2)$ is a continuous, increasing function of θ , that is a bijection from $[0, \pi]$ to $[0, \Delta V(H(c), r_1, r_2)]$. The same result holds for 2-piecewise linear sets of parameter θ .*

Proof of Lemma 4. Let $r_2 > r_1 > 0$, $c > 0$. Let $\mathcal{C}(c, \theta)$ be the cone of revolution of peak c and angle θ . Let $\mathcal{B}_\theta(r_1, r_2) = \mathcal{C}(c, \theta) \cap B_2^d(0, r_2) \setminus B_2^d(0, r_1)$ and $\mathcal{A}(r_1, r_2) = H(c) \cap B_2^d(0, r_2) \setminus B_2^d(0, r_1)$.

First note that $\text{Vol}(\mathcal{B}_\theta(r_1, r_2)) = \text{Vol}(\mathcal{C}(c, \theta) \cap B_2^d(0, r_2)) - \text{Vol}(\mathcal{C}(c, \theta) \cap B_2^d(0, r_1)) = \Delta V(\mathcal{C}(c, \theta), r_1, r_2)$, and similarly $\text{Vol}(\mathcal{A}(r_1, r_2)) = \Delta V(H(c), r_1, r_2)$

To compute the volume of $\mathcal{B}_\theta(r_1, r_2)$, we must cut the integral into three zone: where the bound is the cone, and where it is the surface of either of the balls. There exist a constant K (dependent on the dimension, and containing the integration in all the variables ϕ_i in hyper-spherical coordinates) such as:

$$\begin{aligned} \text{Vol}(\mathcal{B}_\theta(r_1, r_2)) &= \text{Vol}(\mathcal{C}(c, \theta) \cap B_2^d(0, r_2) \setminus B_2^d(0, r_1)) & (96) \\ &= \frac{1}{K} \left[\int_{x=r_1 \cos \theta}^{r_1} \int_{\sqrt{r_1^2 - x^2}}^{x \tan \theta} \rho^{d-2} \, d\rho \, dx + \right. \\ &\quad \left. \int_{r_1}^{r_2 \cos \theta} \int_{\rho=0}^{x \tan \theta} \rho^{d-2} \, d\rho \, dx + \int_{r_2 \cos \theta}^{r_2} \int_{\rho=0}^{\sqrt{r_2^2 - x^2}} \rho^{d-2} \, d\rho \, dx \right] & (97) \end{aligned}$$

It follows that $\text{Vol}(\mathcal{B}_\theta(r_1, r_2))$ is a continuous function of θ .

Furthermore, if $\theta_2 > \theta_1$, then $\mathcal{C}(c, \theta_1) \subset \mathcal{C}(c, \theta_2)$, so $\text{Vol}(\mathcal{B}_{\theta_1}(r_1, r_2)) \leq \text{Vol}(\mathcal{B}_{\theta_2}(r_1, r_2))$, and the function is increasing.

For $\theta = 0$, $\text{Vol}(\mathcal{B}_\theta(r_1, r_2)) = 0$, and for $\theta = \frac{\pi}{2}$, $\mathcal{B}_{\theta_1}(r_1, r_2) = \mathcal{A}(r_1, r_2)$. Hence the result. \square

Proof of Proposition 2. This is an immediate consequence of lemma 4 : From the information of two noises, we can perfectly identify the parameter θ , and thus compute the perfect certificate as $\mathbb{P}_{X \sim q_0(x)} [X + \epsilon e_1 \in \mathcal{C}(0, \theta)]$. \square

C Proofs of Section 4

C.1 Proof of Lemma 1

Lemma 1 (Generalized Neyman-Pearson lemma Chernoff and Scheffe [8]). *Let q_0, \dots, q_n be probability density functions. For any $k_1, \dots, k_n > 0$, we define the Neyman-Pearson set $\mathcal{S}_K = \{q_0(x) \leq \sum_{i=1}^n k_i q_i(x)\}$ and the associated Neyman-Pearson function:*

$$\Phi_K = \mathbb{1} \{ \mathcal{S}_K \}$$

Then for any function $\Phi : \mathcal{X} \rightarrow [0, 1]$ such that $\int \Phi q_i \, d\mu \geq \int \Phi_K q_i \, d\mu$ for all $i \in \{1, \dots, n\}$, we have:

$$\int \Phi_K q_0 \, d\mu \leq \int \Phi q_0 \, d\mu$$

Proof of Lemma 1. By definition of $\Phi_{\mathcal{K}}$, we have:

$$\int (\Phi - \Phi_{\mathcal{K}})(q_0 - \sum_{k=1}^n k_i q_i) d\mu \geq 0 \quad (98)$$

since the integrand is always positive. Hence:

$$\int (\Phi - \Phi_{\mathcal{K}})q_0 d\mu \geq \sum_{k=1}^n k_i \int (\Phi - \Phi_{\mathcal{K}})q_i d\mu \quad (99)$$

Since $\int (\Phi - \Phi_{\mathcal{K}})q_i d\mu \geq 0$, we have:

$$\int (\Phi - \Phi_{\mathcal{K}})q_0 d\mu \geq 0 \quad (100)$$

which is the desired result. \square

C.2 Proof of Theorem 2

Theorem 2 (General approximation theorem). *Let q_0 be the uniform noise on the ℓ_∞ ball $B_\infty(0, r)$ for some $r > 0$. For any $\epsilon > 0$, $\xi > 0$ and $x \in \mathbb{R}^d$, there exists a finite family \mathcal{Q} of probability density functions such that:*

$$\text{NC}(h, q_0, x, \epsilon, \mathcal{Q}) \geq \text{PC}(h, q_0, x, \epsilon) - \xi$$

Proof of Theorem 2. Let $n > 0$, and some $x \in \mathcal{X}$. We can construct a grid of $(n(r + 2\epsilon))^d$ disjoint squares of side size $\frac{1}{n}$, of the form $[\frac{a_1}{n}, \frac{a_1+1}{n}] \times \dots \times [\frac{a_d}{n}, \frac{a_d+1}{n}]$ (except the ones on the border of the ball that are closed) that will cover the ball $B_\infty^d(x, r)$, as well as its translation by ϵ in any direction.

Let us call the squares in this grid A_j for $j = 1 \dots m$ and $m = (\frac{d+2\epsilon}{n})^d$. They all have the same volume $V_n = (\frac{1}{n})^d$.

The idea of this proof is to construct a noise-based classifier that returns 1 only on the squares that are entirely contained in the decision region, *i.e.* a strict underestimate of the true classifier. As the grid gets thinner, the approximation will then converge to the true classifier as a Riemann sum.

Let q_j denote the probability density function of the uniform noise over A_j :

$$\forall j \in \{1, \dots, m\}, z \in \mathbb{R}^d, q_j(z) = \frac{1}{V_n} \mathbb{1}_{z \in A_j} \quad (101)$$

Let $V = \text{Vol}(B_\infty^d(0, r))$. For $j \in \{1, \dots, m\}$, let $p_j = \int h(z)q_j(z)dz$ be the expected response of the true classifier h to noise q_j (*i.e.* what is observed), and the coefficients k_j such that:

$$k_j = \begin{cases} \frac{V_n}{V} & \text{if } p_j = 1, \text{ i.e., } h = 1 \text{ almost surely on } A_j \\ 0 & \text{otherwise.} \end{cases} \quad (102)$$

We choose these specific coefficients to only "activate" the squares where $h = 1$ almost surely, *i.e.* that are entirely inside of the decision region.

Let δ be any attack vector of norm ϵ , and $\tilde{q}_0 = q_0(\cdot - \delta)$ be the distribution after attack by δ . The support of \tilde{q}_0 is $B_\infty^d(-\delta, r)$ which is fully contained in $\bigcup_{i=1}^m A_i$.

Let $\Phi_{\mathcal{K}}$ be the Neyman-Pearson function defined by the $\mathcal{K} := \{k_1, \dots, k_n\}$:

$$\Phi_{\mathcal{K}}(x') = \begin{cases} 1 & \text{if } \tilde{q}_0(x') \leq \sum_{i=1}^n k_i q_i(x') \\ 0 & \text{otherwise} \end{cases} \quad (103)$$

We know that $\Phi_{\mathcal{K}} = 1$ outside of $B_{\infty}^d(x + \delta, r)$ since $\tilde{q}_0 = 0$ there. Let $x' \in B_{\infty}^d(x + \delta, r)$. The A_i are disjoint and cover the ball, so there is exactly one j such that $x' \in A_j$. We then have for any $x' \in A_j$:

$$\Phi_{\mathcal{K}}(x') = \begin{cases} 1 & \text{if } h = 1 \text{ almost surely on } A_j \\ 0 & \text{otherwise} \end{cases} \quad (104)$$

Hence $\Phi_{\mathcal{K}}|_{A_j} = \text{ess inf}_{A_j}(h)$, since h has values in $\{0, 1\}$. It follows that:

$$\int \Phi_{\mathcal{K}}(z) \tilde{q}_0(z) dz = \sum_{i=1}^m (\text{ess inf}_{A_j}(h)) \text{Vol}(A_i \cap B_{\infty}^d(x - \delta, r)) \quad (105)$$

That is a lower Riemann sum for the integral $\int_{B_{\infty}^d(x - \delta, r)} h$, and so converges to it when $m \rightarrow \infty$ as h is Riemann integrable. Hence we can choose n such that, for any δ ,

$$\int \Phi_{\mathcal{K}}(z) \tilde{q}_0(z) dz \leq \int h(z) \tilde{q}_0(z) dz + \xi \quad (106)$$

which gives us the desired result, since this is true for any δ . \square

D Proofs of Section 5

D.1 Proof of Theorem 3

Theorem 3 (Gathering information from gaussian noises). *Let q_0 be any isotropic probability distribution, $\sigma_1, \dots, \sigma_n > 0$. For $i = 1 \dots n$ let $q_i \sim \mathcal{N}(0, \sigma_i)$ be the noises used for information gathering. Let $S_{k_1 \dots k_n}$ be the corresponding Neyman-Pearson set, for any combination of parameters $k_1, \dots, k_n > 0$. Then $\mathbb{P}[\mathcal{N}(0, \sigma_i^2) \in S_{k_1 \dots k_n}]$ can be computed using a Monte Carlo sampling in dimension 2 from a χ distribution with $d - 2$ degrees of freedom.*

Proof of Theorem 3. Let $x \in \mathbb{R}^d$. q_0 is an isotropic probability density function, which means that there exists a function p_0 such that $\forall x \in \mathbb{R}^d, q_0(x) = p_0(\|x\|^2)$. For $i = 1 \dots n$, we have:

$$\mathbb{P}[\mathcal{N}(x, \sigma_i^2) \in S_{k_1, \dots, k_n}] = \frac{1}{(2\pi)^{\frac{d}{2}} \sigma_0^d} \int_{\mathbb{R}^d} \exp\left(-\frac{\|u - x - \delta\|^2}{2\sigma_0^2}\right) \mathbb{1}_{u \in S_{k_1, \dots, k_n}} du \quad (107)$$

where \mathcal{S} is the Neyman-Person set defined as:

$$\mathcal{S}_{k_1, \dots, k_n} = \left\{ u \in \mathbb{R}^d \mid p_0(\|u - x - \delta\|^2) \leq \sum_{i=0}^n k_i \exp\left(-\frac{\|u - x\|^2}{2\sigma_i^2}\right) \right\} \quad (108)$$

Where the k_i are defined as in Corollary 1.

By expressing Equation (107) with hypercylindrical coordinates of center x and axis δ , we have:

$$\mathbb{P}[\mathcal{N}(x, \sigma_i^2) \in S_{k_1, \dots, k_n}] = \frac{1}{(2\pi)^{\frac{d}{2}} \sigma_i^d} \int_{\mathbb{R}^d} \exp\left(-\frac{\|u - x\|^2}{2\sigma_i^2}\right) \mathbb{1}_{x \in \mathcal{S}} dx \quad (109)$$

$$= \frac{1}{(2\pi)^{\frac{d}{2}} \sigma_0^d} \int_{\substack{\mu \in \mathbb{R} \\ r \in \mathbb{R}^+ \\ \phi_1, \dots, \phi_{d-3} \in [-\pi, \pi] \\ \phi_{d-2} \in [0, 2\pi]}} \exp\left(-\frac{r^2 + \mu^2}{2\sigma^2}\right) \mathbb{1}_{(r, \mu) \in \tilde{\mathcal{S}}^J} dr d\mu d\phi_1 \dots d\phi_{d-2} \quad (110)$$

where from Blumenson [5], the Jacobian J of the change of variables is:

$$J = r^{d-2} \prod_{k=1}^{d-2} \sin^k \phi_{d-1-k} \quad (111)$$

and where $\tilde{\mathcal{S}}$ is the updated Neyman-Person set:

$$\tilde{\mathcal{S}} = \left\{ r, \mu \in \mathbb{R} \mid p_0(r^2 + (\mu - \epsilon)^2) \leq \sum_{i=0}^n k_i \exp\left(-\frac{r^2 + \mu^2}{2\sigma_i^2}\right) \right\} \quad (112)$$

Given that the indicator function is independent of the $\phi_1, \dots, \phi_{d-2}$, we can rearrange the above equation as follows:

$$\begin{aligned} \mathbb{P} [\mathcal{N}(x, \sigma_i^2) \in \mathcal{S}_{k_1, \dots, k_n}] &= \frac{1}{(2\pi)^{\frac{d}{2}} \sigma_i^d} \left(\int_{\substack{\mu \in \mathbb{R} \\ r \in \mathbb{R}^+}} \exp\left(-\frac{r^2 + \mu^2}{2\sigma^2}\right) r^{d-2} \mathbb{1}_{(r, \mu) \in \tilde{\mathcal{S}}} dr d\mu \right) \\ &\quad \left(\int_{\substack{\phi_1, \dots, \phi_{d-3} \in [-\pi, \pi] \\ \phi_{d-2} \in [0, 2\pi]}} \prod_{k=1}^{d-2} \sin^k \phi_{d-1-k} d\phi_1 \dots d\phi_{d-2} \right) \end{aligned} \quad (113)$$

By setting A as:

$$A = \int_{\substack{\phi_1, \dots, \phi_{d-3} \in [-\pi, \pi] \\ \phi_{d-2} \in [0, 2\pi]}} \prod_{k=1}^{d-2} \sin^k \phi_{d-1-k} d\phi_1 \dots d\phi_{d-2} \quad (114)$$

we have:

$$\mathbb{P} [\mathcal{N}(x, \sigma_i^2) \in \mathcal{S}_{k_1, \dots, k_n}] = \frac{A}{(2\pi)^{\frac{d}{2}} \sigma_0^d} \left(\int_{\mu \in \mathbb{R}} \int_{r \in \mathbb{R}^+} \exp\left(-\frac{r^2}{2\sigma_0^2}\right) \exp\left(-\frac{\mu^2}{2\sigma^2}\right) r^{d-2} \mathbb{1}_{(r, \mu) \in \tilde{\mathcal{S}}} dr d\mu \right) \quad (115)$$

Finally, we can express this probability with an expected value over a Gaussian and Chi distribution:

$$\mathbb{P} [\mathcal{N}(x, \sigma_i^2) \in \mathcal{S}_{k_1, \dots, k_n}] = \mathbb{E}_{\substack{\mu \sim \mathcal{N}(0, \sigma_i^2) \\ r \sim \chi(d-1, 0, \sigma_i^2)}} \left[\mathbb{1}_{(r, \mu) \in \tilde{\mathcal{S}}} \right] \quad (116)$$

which concludes the proof. \square